Received: November 18, 2022. Revised: February 22, 2023.

INASS

International Journal of
Intelligent Engineering & Systems

http://www.inass.org/

Detection and Diagnosis of Diabetic Retinopathy Using Transfer Learning Approach

M. Vamsi Krishna[1] **B. Srinivasa Rao[1]***

[1]*School of Computer Science & Engineering (SCOPE), VIT-AP University, Amaravati, Andhra Pradesh, India*
* Corresponding author's Email: srinivasarao34743@gmail.com

Abstract: The human eye's anatomical features and defects can be captured by using the retinal image modality known as fundus imaging. The effective method for observing and detecting a variety of ophthalmological diseases is fundus imaging. Diseases including diabetic retinopathy, diabetic macular edema (DME), glaucoma, and cataracts are indicated by changes in and around the structural abnormalities like macula, optic disc, blood vessels, and fovea. More than one retinal disease may be present in one or both of the patient's eyes. For multi-class fundus image classification, the new deep learning (DL) model is proposed for ophthalmological diseases using a transfer learning (TL) based deep identification network (DeepID3) network. The flower pollination optimization algorithm (FPOA) is used to optimize the hyperparameters of the network. The model is tested using many large public datasets. The best pre-trained convolutional neural network (CNN) models from ImageNet were used in the experiment. Different performance optimization strategies were also used. Multi-class multi-label fundus image classification is more effective while using the DeepID3 net pre-trained architecture with FPOA optimizer. Maximum accuracy of 99.23%, sensitivity of 98%, precision of 98.13%, recall of 98%, F1-score of 98.3%, and specificity of 98.28% were attained by the proposed model for multi-class classification. The implementation is done by using the Python platform. The performance of the proposed approach is demonstrated by extensive experiments and comparison with baseline methods.

Keywords: Fundus images, Transfer learning, Multi-class classification, Hyperparameters.

1. Introduction

People with diabetes may experience one of the eye diseases known as diabetic eye disease (DED); these diseases include cataracts (Ca), glaucoma (Gl), DME, and diabetic retinopathy [1]. Long-term eye damage based on diabetes can cause vision impairment or even blurred vision [2]. The DED can be avoided and stopped from getting worse by monitoring diabetes [3]. The possibility of having a DED diagnosis is about one-third of those with diabetes [4]. The World Health Organization (WHO) has determined that 2.2 billion people worldwide have vision loss or are blind, and there are potentially treatable vision problems in at least 1 billion people [5]. The first step in treating these diseases is recognizing and diagnosing them [6].

Visual impairments and retinal diseases are effectively implemented by developing multiple detection and preventative methods [7]. From the retinal fundus, retinal eye disorders are detected using the DL methods that significantly improve many practical applications [8, 9]. For binary classification of multiple eye disease retinal fundus images, high performance has been attained by DL approaches [11, 12]. However, the type of various classes of retinal eye diseases is still a challenge.

For binary classification of normal and disease, the DL has typically obtained significant recognition accuracies [12]. However, for the multi-class classification of normal and disease, the performance of DL could be more attractive, especially for impairment at an early stage. To distinguish between normal images and diseased pathologies, an efficient deep convolutional neural network (DCNN) for the DED classification model is developed [13, 14]. In the proposed work, different DCNN architectures are evaluated to determine the framework that offers the most outstanding performance for the DED

classification tasks for multi-class classification [15].

Adequate medical image detection and classification findings have already been established and validated using pre-trained models or transfer learning (TL) methods [16, 17]. Following the TL standard, the most recent CNN models are used to conduct this research that had been pre-trained with the large public image repository ImageNet [18, 19]. For multi-class classification, the publically available fundus images are used to train the network model's top layers with initialized weights [20].

The research presented in this study is focused on various DED cases, which are more difficult to classify than in the past. Initially, the best-performing CNN model selection is based on a comprehensive experiment. This evaluates the number of specific enhancements, such as contrast enhancement and optimizer selection. Among the at-risk population, the performance of mass screening services is enhanced by developing an effective, efficient, and completely automated DL-based system [16, 17].

For classification, generalization capabilities and high performance of DL methods are incorporated by the proposed method. Several categories of ophthalmological diseases are classified from fundus images by developing the transfer learning-based pre-trained DeepID3 network with an FPOA optimizer.

The significant contributions of the proposed research are as follows:

- For image pre-processing, contrast enhancement is accomplished by applying mathematical morphology processes in the retinal fundus images.
- The transfer learning-based DeepID3 network is then proposed for classifying fundus images into different classes of ophthalmological diseases, including cataracts, glaucoma, DME, and diabetic retinopathy.
- Next, the CNN hyperparameters are optimized by using FPOA. It is used for achieving high classification accuracy while diagnosing different diseases.
- The DRISHTI-GS, Messidor-2, Messidor, and retina datasets are used to assess the proposed model. Python is the platform used for experiments. According to the experimental results, the proposed DeepID3 net-FPOA model outperforms the previous techniques.

The research is structured as follows, the existing approaches for classifying fundus images are discussed in section 2. The proposed transfer learning-based algorithms for classifying fundus images are described in section 3. The experimental evaluation and performance of the proposed algorithm are discussed in section 4. Section 5 concludes the paper.

2. Literature survey

This section reviews some existing DL techniques for diagnoses of diabetic retinopathy disease.

For blood vessels (BV) and optic disc (OD) segmentation, [21] proposed two different U-Net models in this research. After the extraction of BV and OD, the improved retinal images are fed to the transfer learning-based model VGGNet in the second stage. The retinal biomarkers are identified by the proposed method for the detection of diabetic retinopathy, including exudates (EX), hemorrhages (HM), and microaneurysms (MA).

In this study, Kaur et al. established a classification scheme for retinal images that consists of three main blocks. In original images, the denoising convolution neural network (DnCNN) and contrast limited adaptive histogram equalization (CLAHE) technique are initially used to pre-process the images to eliminate the induced noise. After pre-processing, the K-means algorithm is used for the segmentation process. After segmentation, the images are loaded into the proposed transfer learning-based EyeNet model.

For detecting diabetic retinopathy, a new deep transfer learning model is proposed by Khalifa et al. [23]. The 2019 dataset from the asia pacific tele-ophthalmology society (APTOS) was used to train and test the DL models. VGG19, VGG-16, GoogleNet, SqueezeNet, ResNet18, and AlexNet were the deep transfer models selected for this research. The chosen models have the lowest layers than the larger ones, like InceptionResNet and DenseNet. Overfitting problem-solving and model strengthening is performed using data augmentation methods in this research.

A novel hybrid DL technique is proposed by Gangwar et al. [24] for solving the problem of the detection of diabetic retinopathy in this research. The transfer learning-based pre-trained InceptionResNetV2 is used to detect diabetic retinopathy. The proposed network model consists of a block of CNN layers for processing the network.

A transfer learning-based technique is developed by Smadi et al. [25] to accurately decide the level of diabetic retinopathy severity. Diabetic retinopathy is detected using multiple pre-trained CNN models with

Table 1. Literature survey

Reference	Year	Dataset	Model	Benefits	Difficulties
Bilal et al. [21]	2022	EyePACS-1, Messidor-2,and DIARETDB0	Transfer learning-based VGGNet model	(i) It generates reliable solutions with high sensitivity and specificity (ii) It detects the images more fastly	(i)It reduces the classification performance (ii)It reduces the quality of classification in real-time applications
Kaur et al. [22]	2021	DRIVE and STARE	Transfer learning-based EyeNet model	(i)It effectively extracts multi-level features of the image (ii) This model can be diagnosed quickly and precisely	(i) Powerful hardware is needed for fast prediction results. (ii) It Requires additional time for training
Khalifa et al. [23]	2019	APTOS 2019	AlexNet model	(i) The overfitting problem of the network is resolved. (ii) It is effective at accurately identifying and categorizing disease lesions.	(i) Complex training (ii) The network model is unreliable and difficult to interpret
Gangwar et al. [24]	2021	Messidor-1 and APTOS 2019	Inception-ResNet-v2	(i) It effectively classifies the disease images (ii) The trainable parameters are drastically decreased.	(i) In situations where the number of classes is very high, it will lose accuracy in classification.
Smadi et al. [25]	2021	APTOS 2019	Inception-V3+GAP-based classifier	(i) Interscale variations are successfully captured. (ii) Faster image detection is achieved.	(i) It reduces the classification accuracy (ii) High computer resources are required for training with high-resolution data.
Houby et al. [26]	2021	Kaggle dataset	Transfer learning-based VGG-16 model	It solves the overfitting problem of the network	(i) It does not accurately classify low-intensity, and noisy data images (ii) The feature extraction approach is not suitable for accurate detection

the global average pooling (GAP) approach. A different CNN method is proposed by Houby et al. [26] to detect and classify diabetic retinopathy and its stages in the colored retinal fundus images. CNN can automatically diagnose eye conditions by identifying complex structures on the retina. For detection and classification, the pre-trained VGG-16 CNN model is used in this research.

To overcome the difficulties of the existing models on multi-class DED detection and classification, we propose a new transfer learning-based approach.

3. Proposed methodology

The multi-class DED detection and classification are improved using the proposed method with experimental evaluation of many classification enhancement methods. This is the main objective of this proposed system. The retinal fundus images are classified into five classes: Normal, Ca, Gl, DME, and DR (multi-class classification). Data from publicly accessible open-source databases, such as the DRISHTI-GS, Messidor-2, Messidor, and the retina datasets, were used. The contrast enhancement for image pre-processing is achieved by using mathematical morphological processes in the retinal fundus images. We have proposed a DeepID3 network for classifying multiple DED diseases. The hyperparameters are optimized by the FPOA optimizer. The schematic diagram of the proposed method is given in Fig. 1.

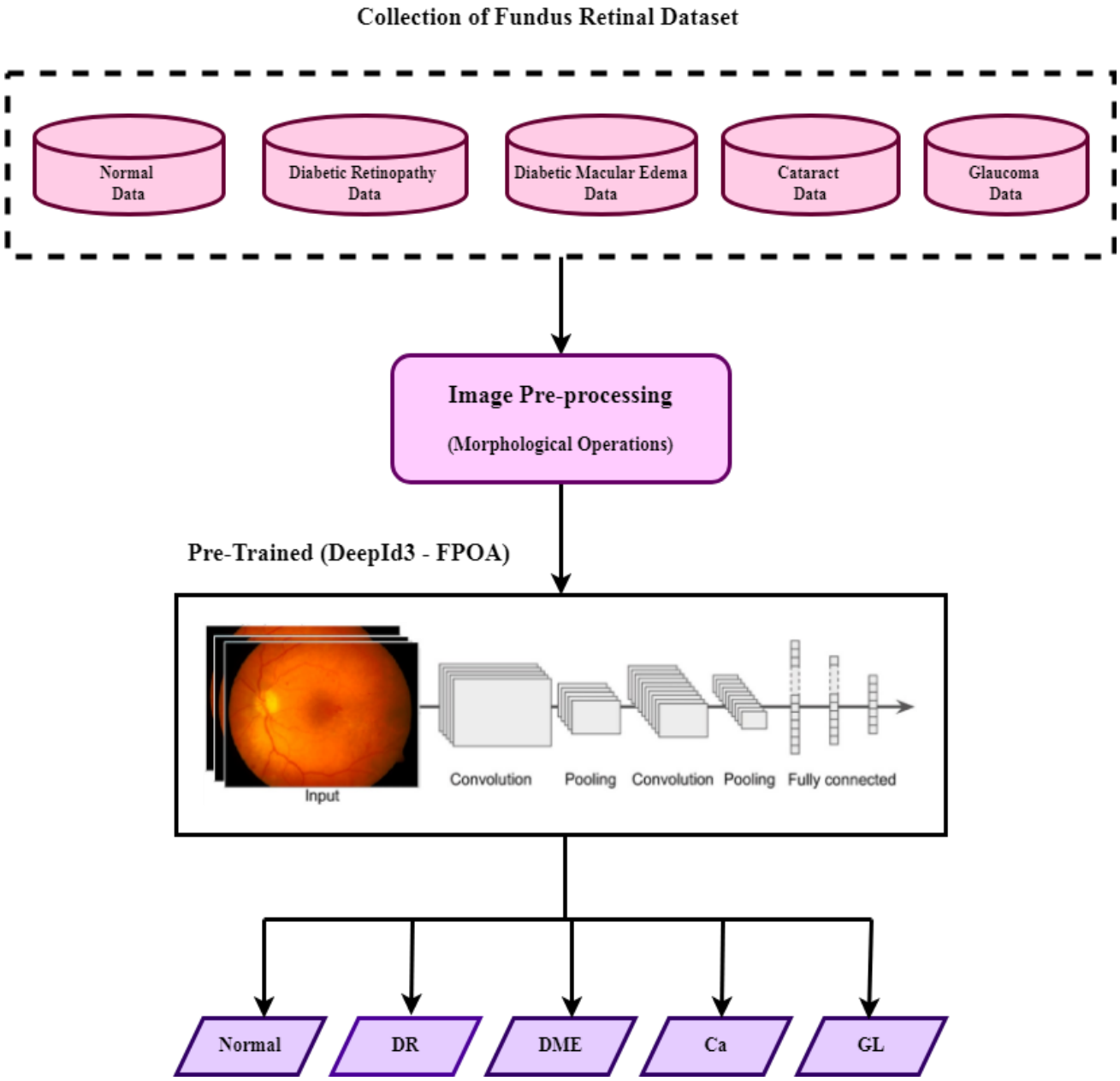

Figure. 1 Schematic diagram of the proposed methodology

3.1 Data collection

The publicly accessible DRISHTI-GS, Messidor-2, Messidor, and retina datasets were used from open-source databases. Despite the Messidor dataset being significantly small scale, the dataset has high-fidelity images with reliable labeling. Similarly, Messidor-2 is utilized by different individuals to assess the performance of the DED algorithm. The 1748 images representing 874 other subjects are in the database. The initial Messidor data set of 1200 images is different from Messidor-2. Each item is represented by two images, one for each eye. The DRISHTI-GS collection has 101 retinal images, including 70 lesion images and 31 normal images. The retina dataset on GitHub was used to create the cataract dataset. A total of 100 cataract images are present in this dataset. The data distribution is given in Fig. 2.

3.2 Image pre-processing

Mathematical morphology has been utilized to enhance contrast in retinal fundus images. The structural qualities of objects serve as the foundation for mathematical morphology methods. The input for morphological operators consists of two sets of data. The first set contains the original image, while the mask-type structural element (SE) is shown in the second set. The mask is a 1's and 0's valued matrix,

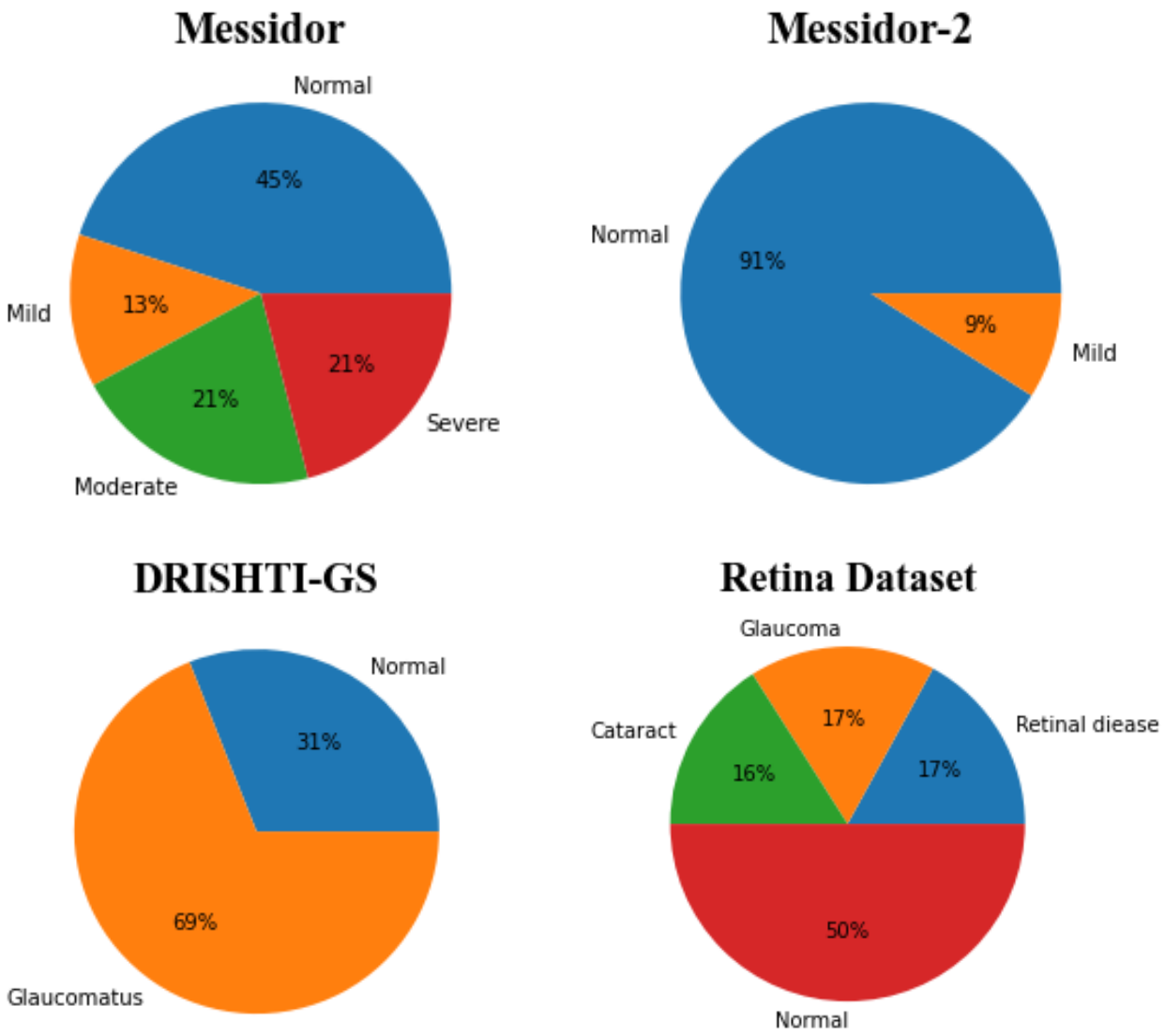

Figure. 2 Data distribution in various datasets

and the source image is in binary or grey level. The erosion and dilation operators in morphological operators are described by Eqs. 1 and 2, which were IM(x,y) to represent the gray-level image matrix id and SE(m,n) represent SE.

$$IM\Theta SE = \min_{m,n}\{IM(x+m, y+n) - SE(m,n)\} \quad (1)$$

$$IM \oplus SE = \max_{m,n}\{IM(x-|m, y-n) + SE(m,n)\} \quad (2)$$

The size of the object is decreased, and the size of an image's holes is increased by using the erosion operator. Minimal information is also eliminated by using this operator. The bright areas under the SE are removed by darkening the final image relative to the source image. The dilation operator performs the reverse function of the erosion operator. The object's size is increased, and image holes are decreased by using the dilation operator. As a result, applying the dilation and erosion operations to the same image yields the opening operator comparable to equation 3. In contrast, the closing operator performs the reverse operation and yields Eq. 4.

$$IM \circ SE = (IM\Theta SE) \oplus SE \quad (3)$$

$$IM \bullet SE = (IM \oplus SE)\Theta SE \quad (4)$$

Where $IM \circ SE$ represents the opening operator and $IM \bullet SE$ represents the closing operator.

$IM\Theta SE$ indicates erosion operation and $IM \oplus SE$ indicates dilation operation.

The opening operator fills the small gaps and the bad relationships among small information and objects. The SE's shape and size are often determined randomly; however, the disk-shaped SE is applied

more commonly for medical images.

3.3 Classification using DeepID3 net

The pre-trained CNNs are used for incorporating the DED dataset classification in this proposed work. The particular feature representations without losing knowledge of the structural features are obtained by converting the feature vector with a specified weight matrix using a deep convolutional neural network (DCNN). The system targets jobs by reusing elements discovered on the source task. TL is helpful in fields of research that require substantial computer resources and vast amounts of data. As a result, the best classification results are produced by developing the pre-trained models. Detailed information on the pre-trained models is represented in this section.

A few characteristics are inherited by the proposed DeepID3 net, such as neural weights not shared in the feature extraction layers and the procedure for incorporating supervisory signals into early layers. In contrast to other networks, the DeepID3 net has ten to fifteen non-linear feature extraction layers, considerably increasing in depth. Before each pooling layer, several convolution/inception layers are stacked to increase the depth of the DeepID3 network. While limiting the parameter's range, the features with more complex non-linearity and more significant receptive fields are formed using the continuous convolution/inception layers.

Before each pooling layer, two continuous convolutional layers are added to the proposed DeepID3 network. Several full connection layers branching from intermediate layers have additional supervisory signals, which are used for effective optimization and efficient mid-level feature learning. Features with a smaller feature dimension and greater expressiveness are provided by top layers with unshared parameters. The last locally connected layer of the DeepID3 net is used to extract the final features without an additional fully connected layer.

Except for the pooling layers, all layers in the proposed network use rectified linear non-linearity. And in the final feature extraction layer, dropout learning is added. The GoogLeNet and VGGNet networks are more significant than the proposed DeepID3 networks in object recognition because the proposed DeepID3 networks have a limited amount of feature mappings in each layer. The proposed model learns the features using the Joint Bayesian model for multiple DED classification and detection.

3.4 Parameters optimization using FPOA

The loss function is reduced by updating the parameters of the network in the training phase. However, the optimizer used significantly impacts the size and direction of the parameter adjustment. The optimizer performance is evaluated by the most significant weights, such as learning rate and regularization. A loss function that is too high or too low in learning rate either fails to converge or falls within the local minimum's range rather than the absolute minimum. While regularization prevents the significant weighting elements from making accurate predictions, it also prevents the model from overfitting. As a result, when exposed to new data, the classifier's capacity for generalization improves. FPOA optimization algorithm is used for the experiments.

Using FPOA optimization techniques, the proposed network model's weight variation is optimized. Based on the natural pollination of flowers, the FPOA was developed. Pollen is often transferred from a plant's male to female parts during flower pollination. Self-pollination and cross-pollination are two different types of pollination. Cross-pollination is a biological process that requires the help of wind, birds, insects, and water to transfer pollen. The local search is represented by abiotic pollinators, while objects of global search are represented by biotic pollinators using levy flight. $P \in [0,1]$ represents the switching probability. It determines both biotic and abiotic pollination. The following equation represents the flower consistency:

$$e_i(t+1) = e_i(t) + L(e_i(t) - q^*) \quad (5)$$

Where the present best solution is represented by q^*, pollen i along vector e_i at iteration t is indicated by $e_i(t)$, and levy flight is indicated by L. Algorithm 1 provides information on optimizing hyperparameters using FPOA.

The convergence and accuracy of CNN are significantly dependent on the hyperparameters. Based on CNN, network hyperparameters were selected. Learning rate, momentum, number of epochs, and regularization coefficient are the typical CNN training hyperparameters. SGD with momentum (SGDM) is a method that helps accelerate gradient vectors in the right directions, thus leading to faster converging. The weight updates are controlled by a momentum based on the previous weight updates, and the learning rate adjusts the gradient descent algorithm's speed. The SGDM operation is performed using the features' weights (W) and bias (b). The number of epochs is represented by the learning algorithm, which updates the network several times with the entire dataset.

Algorithm 1. Hyperparameter optimization using FPOA

Requirement: Number of search agents: k, dimension: d, Batch size: q, Number of iterations for Optimization: t,
hyperparameter evaluation function: Fy, hyperparameters: M1, M2, M3, M4

Initialize Random Flower pollinators population. $e_i(i = 1,2,\dots k)$
Initialize a, A, B

Procedure: Sample a batch of training data
Determine the search consistency probability $p \in [0,1]$.
while the number of optimization iteration
for k=1 to m (m=flowers in the population)
if rand>p, use a Levy flight to determine global pollination
else
choose j and k among the obtained solution and perform local pollination using
$e_i(t+1) = e_i(t) + L(e_i(t) - q^*)$
End if
Obtain new solutions and evaluate their fitness
Check the new solution; if it is better, choose a new solution
Else retain the previous solution
Choose the first three search agents: λ, μ, δ
End if
End for
Update a, A, B
(M1, M2, M3, M4) = hyperparameter evaluation function (Fy)
Update λ, μ, δ
End while
W&b←sgdm (F_y, M1, M2, M3, M4)
End Procedure

Overfitting is avoided by regularization. Consequently, the hyperparameters are optimized to create these configurations. Because of this, the network is better able to get accurate results. The algorithm provides details about hyperparameter optimization using FPOA.

In the proposed system, the classification process is initiated by the fully connected layer, which is the final layer. It exhibits high generalization capabilities for improving the classifier's accuracy.

4. Results

The experimental evaluation is performed by using Python. To address the input needs of each model, the image's size and resolution have both been standardized. Multiple age-related eye diseases are identified by the proposed system. The DeepID3 net-FPOA model using fundus images is developed for classifying diseases like cataracts, glaucoma, DME, and diabetic retinopathy. The DRISHTI-GS, Messidor-2, Messidor, and retina online databases were used to find the fundus images. The dataset images were utilized for testing with 30% of the images and training with 70%. Final scores were validated using the key evaluation metrics for the accuracy, specificity, precision, sensitivity, recall, and F1-score of test data.

4.1. Performance evaluation for classification

The effectiveness of each CNN is assessed using various criteria to determine whether the diagnosed DED is truly or falsely classified in the retinal fundus images, which are then analyzed as follows. First, a confusion matrix was created by developing the cross-validation estimator. The model is effectively classified by associating the model with a particular class, and the true positive (TP) indices comprise all data samples. In the confusion matrix, the true negative (TN) indices have additional samples. These samples are related to other successfully determined classes. The classifier's estimated number of incorrect samples is referred to with the false positive (FP) and false negative (FN) indices in the uncertainty matrix.

For experimental analysis, performance parameters for accuracy are retrieved from the confusion matrix. In Eq. (6), accuracy is the proportion of true negative and true positive values divided by the confusion matrix's total values. In the proposed model, the classifier's performance is determined by the factors of the confusion matrix.

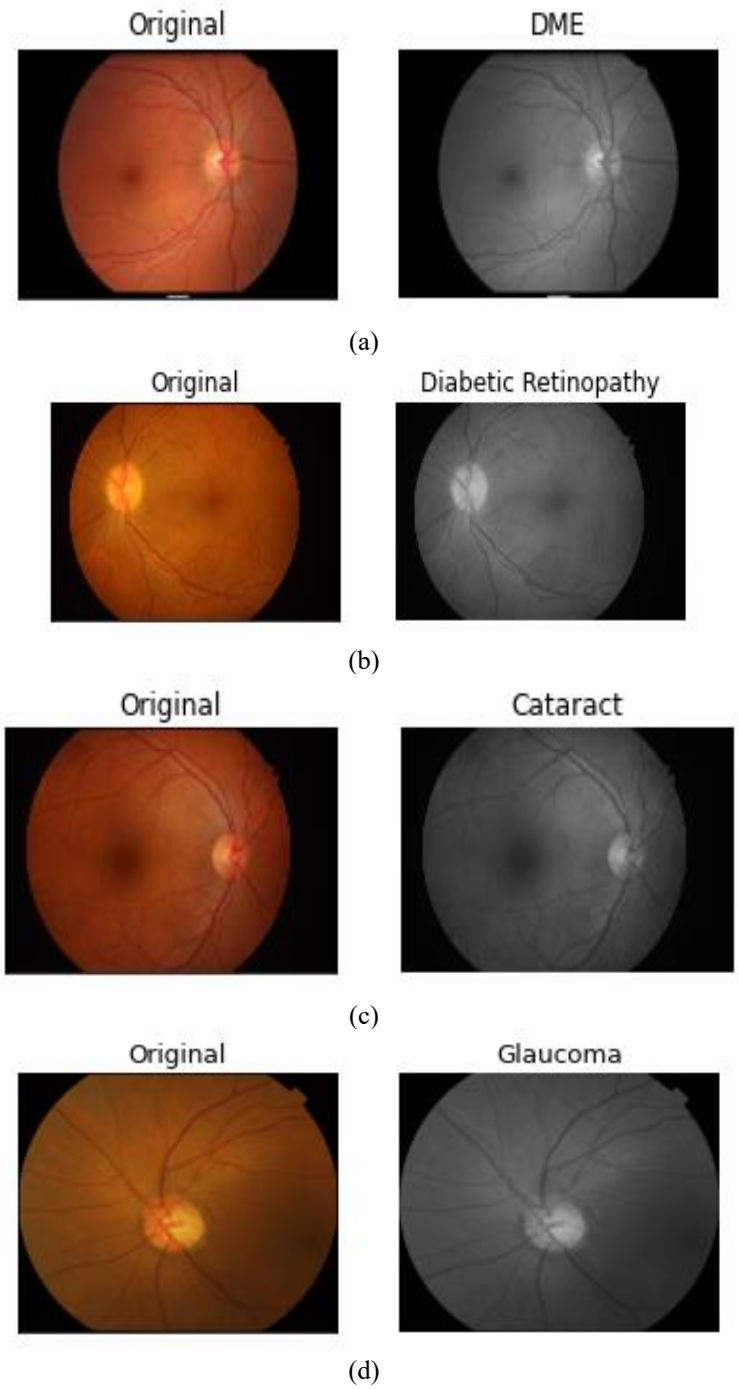

Figure. 3 The outcome of contrast-enhanced images: (a) DME, (b) diabetic retinopathy, (c) cataract, and (d) glaucoma

$$Accuracy(\%) = \frac{TP+TN}{TP+FN+TN+FP} \quad (6)$$

Similarly,

$$Sensitivity = \frac{TP}{TP+FN} \quad (7)$$

$$Pr\,e\,cision = \frac{TP}{TP+FP} \quad (8)$$

$$Specificity = \frac{TN}{TN+FP} \quad (9)$$

$$Re\,c\,all = \frac{TP}{Tp+FN} \quad (10)$$

$$F1 - Score = \frac{2(Re\,call \times Pr\,ecision)}{Re\,call+Pr\,ecision} \quad (11)$$

4.2 Experimental results

Mathematical morphological operations are used to improve the contrast in the retinal fundus images. Fig. 3 shows the original and contrast enhancement images of multiple age-related eye diseases.

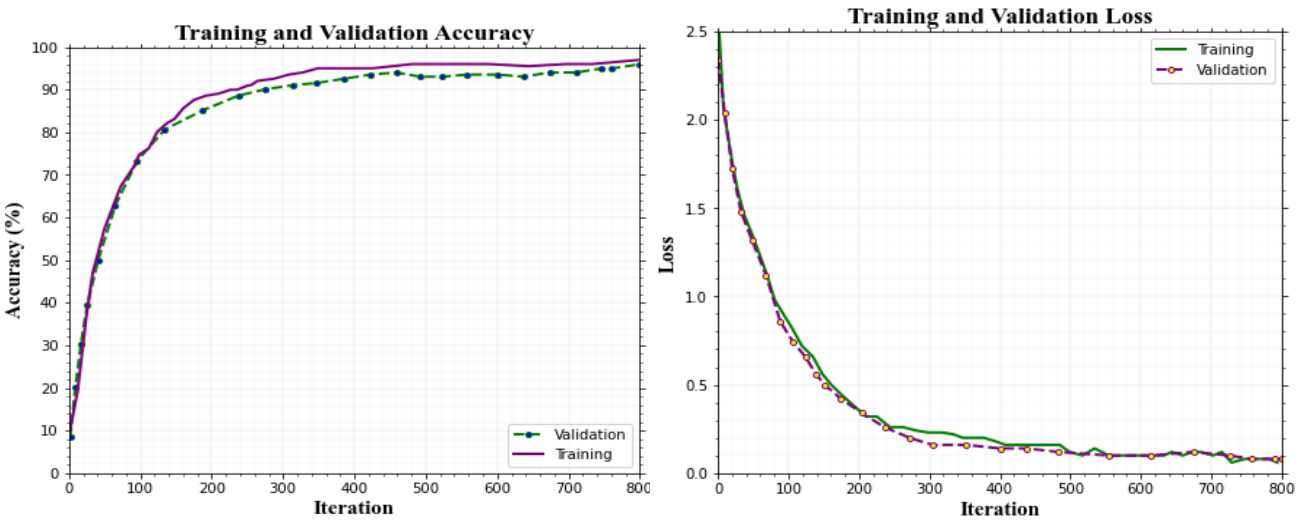

Figure. 4 Accuracy and Loss graph of both training and validation for multi-class classification of eye diseases

Table 2. Metrics of each class's performance for the proposed model

Multiple Diseases	Specificity (%)	Precision (%)	Sensitivity (%)	Recall (%)	F1-score (%)	Accuracy (%)
Normal	98.56	98.28	99.12	98.65	98.09	98.76
Glaucoma	99.28	97.05	98.72	97.77	98.04	99.98
Diabetic Retinopathy	98.92	98.66	99.19	98.31	97.98	98.54
DME	99.01	98.01	98.43	97.98	98.49	98.67
Cataract	98.28	98.33	97.32	98.33	98.33	98.45

The training phase was conducted with 26 epochs and a learning rate of 0.01 for better results. Each epoch used a total of 31 iterations in the experiment analysis. The accuracy and loss graph of both training and validation accuracy for multiple eye disease classifications is given in Fig. 4. With an accuracy of 99.23%, the training progress was validated. To reach the final iteration, 1 minute 54 seconds timing is used for the entire training process. The images were fed into the 224 x 224 x 3 input layer during the training phase, followed by the two convolution layers for feature extraction. During the training phase, the validation accuracy is improved by selecting hyperparameters.

The confusion matrix values are used for assessing the proposed work's performance for each class. These values are evaluated using sensitivity, precision, accuracy, F1-score, specificity, and recall. The proposed model's confusion matrix and reciever operating characteristic (ROC) curve for multiple DED classes are in Fig. 5. A total of 99.23% accuracy, 98.13% precision, 98% sensitivity, 98% recall, 98.28% specificity, and 98.3 % F1-score were provided by the proposed algorithm.

Table 2 contains a description of the model's class-wise performance for the parameters of specificity, sensitivity, recall, F1 score, and accuracy. The model exhibits enhanced accuracy and better sensitivity. The minority class has a high accuracy rate since there are many more negative samples than positive ones in that group. This represents that the model correctly classified abnormalities for glaucoma and other conditions. The small sample of the validation set's images is employed to determine the class-wise performance. In the proposed work, performance results of the multiple eye disease classes are effectively classified.

5. Discussion

The performance results are compared in Table 3; the proposed method was contrasted with the existing techniques for identifying disorders like DME, glaucoma, normal, cataract, and diabetic retinopathy. It demonstrates a development in the proposed model's capability to identify DED compared to the four distinct optimization strategies. The best results are produced by the proposed DeepID3 net model with an FPOA optimizer configuration. The effectiveness of the proposed method is compared with the recent existing methods such as CNN-RMSprop [27], VGG-16-SGD [28], ResNet-Adam

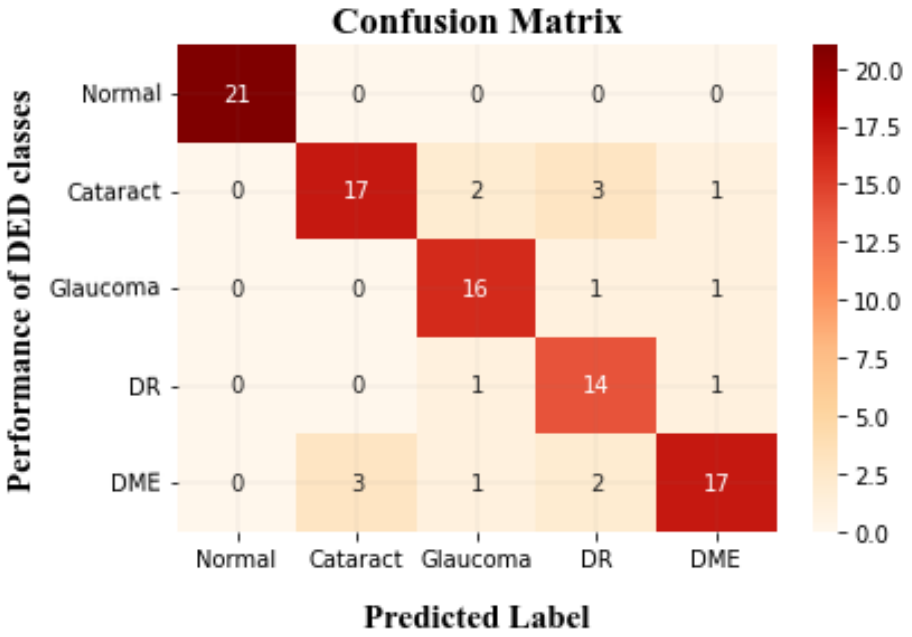

(a)

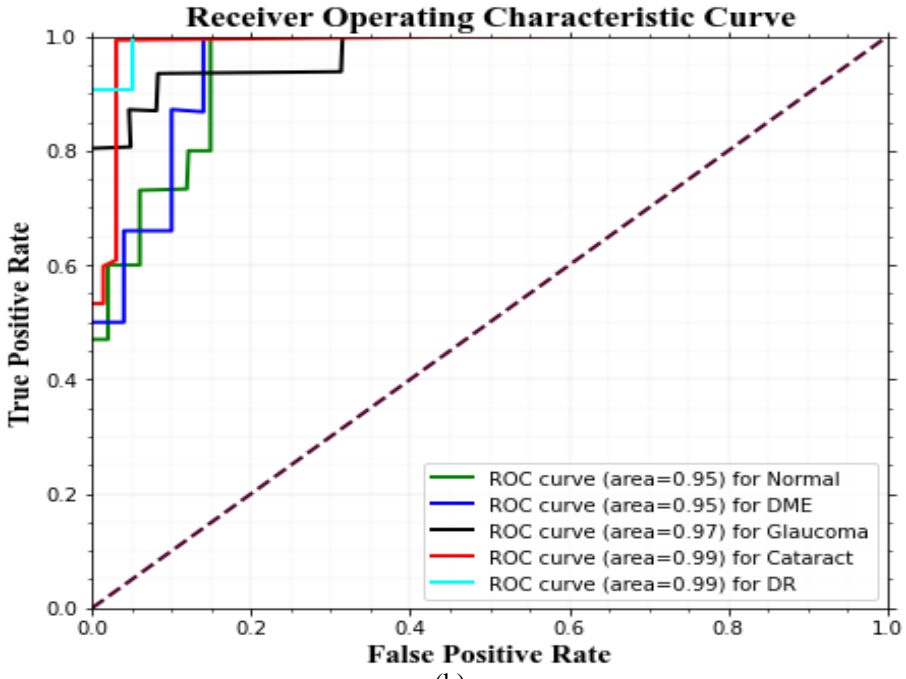

(b)

Figure. 5: (a) Confusion matrix and (b) ROC curve

Table 3. Performance comparison results

Models	F1-score (%)	Recall (%)	Precision (%)	Specificity (%)	Sensitivity (%)	Accuracy (%)
CNN-RMSprop [27]	89.01	85.12	92.25	97.4	92	81.33
VGG-16-SGD [28]	85.57	79.54	80.09	86.45	83.2	87.16
ResNet-Adam [29]	84.15	82.36	90.12	84.62	82	84.92
InceptionV3-Adam [30]	85.37	87.12	83	86.14	90.2	85.6
Proposed Model (DeepID3 net-FPOA)	98.3	98.50	98.13	98.28	98	99.23

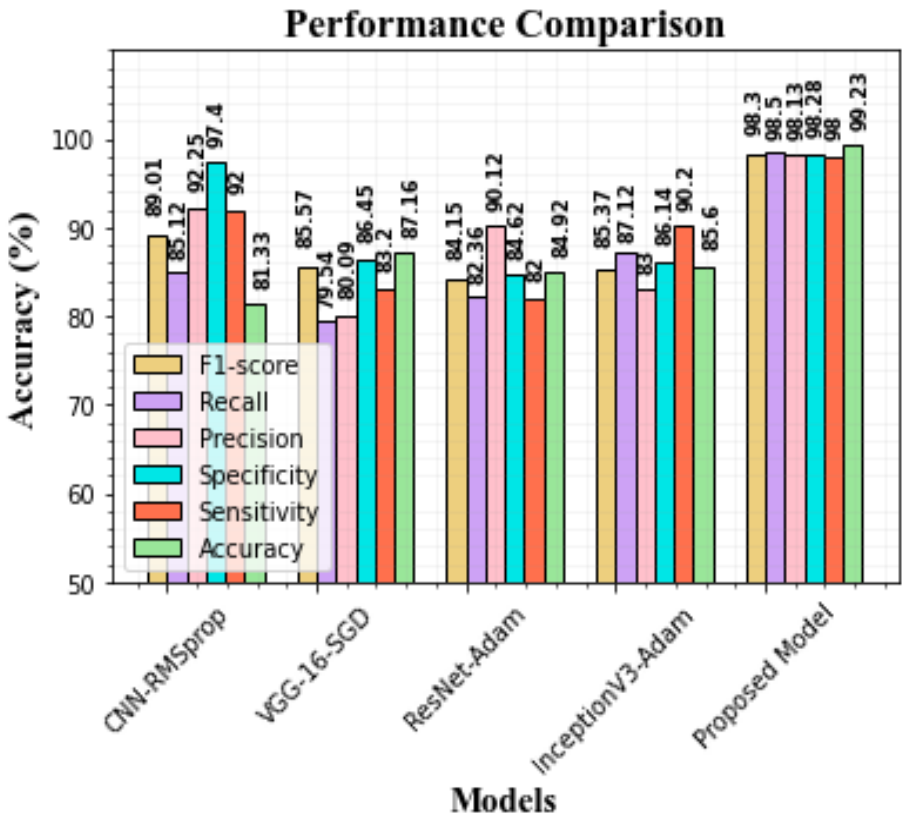

Figure. 6 Performance comparison graph

[29], and InceptionV3-Adam [30]. While compared to the prior deep learning models, the proposed DeepID3 net-FPOA model achieves better results and effectively classifies the multi-class DED classification.

In contrast with the previous research, the proposed DeepID3 network model has a simple framework. The main advantage of using the FPOA optimizer is that it prevented overfitting and had no impact on network performance due to parameter addition. The graphical performance comparison is shown in Fig. 6.

6. Conclusion

For the detection of multi-class DED diseases, the working system proposes a new DeepID3 net-FPOA model based on transfer learning for automated multi-class classification. The proposed methodology uses fundus pictures to classify the various DED disorders, including normal, DME, cataract, glaucoma, and diabetic retinopathy. To implement classification, the proposed work uses combined datasets from multiple sources. Using mathematical morphological processes, contrast enhancement for image pre-processing is achieved. The DeepID3 network was then used to classify it. The FPOA is used to optimize the hyperparameters, and efficiency and accuracy are increased by using this optimizer. While comparing to the other existing deep learning models, the diseased image was more accurately identified by the proposed DeepID3 net-FPOA model with an accuracy of 99.23%. Better performance metrics are provided by the proposed approach in terms of recall, specificity, precision, sensitivity, and F1 score when compared to the previously optimized networks. The results of the proposed method can automatically detect and classify the multiple DED disease classes. This proposed model is used for several clinical applications. For detecting various accurate DED diseases, this method improves healthcare delivery. The performance results of the research indicate improvement of the proposed network model to achieve performance improvements in the future.

Reference

[1] S. Qummar, F. G. Khan, S. Shah, A. Khan, S. Shamshirband, Z. U. Rehman, I. A. Khan, and W. Jadoon, “A deep learning ensemble approach for diabetic retinopathy detection”, *IEEE Access*, Vol. 7, pp. 150530-150539, 2019, //doi.org/10.1109/ACCESS.2019.2947484.

[2] R. Pires, S. Avila, J. Wainer, E. Valle, M. D. Abramoff, and A. Rocha, “A data-driven approach to referable diabetic retinopathy detection”, *Artificial Intelligence in Medicine,*

Vol. 96, pp. 93-106, 2019, doi: 10.1016/j.artmed.2019.03.009.

[3] S. Wan, Y. Liang, and Y. Zhang, "Deep convolutional neural networks for diabetic retinopathy detection by image classification", *Computers & Electrical Engineering*, Vol. 72, pp. 274-282, 2018, doi: 10.1016/j.compeleceng.2018.07.042.

[4] L. Qiao, Y. Zhu, and H. Zhou, "Diabetic retinopathy detection using prognosis of microaneurysm and early diagnosis system for non-proliferative diabetic retinopathy based on deep learning algorithms", *IEEE Access*, Vol. 8, pp. 104292-104302, 2020, //doi.org/10.1109/ACCESS.2020.2993937.

[5] D. J. Hemanth, O. Deperlioglu, and U. Kose, "An enhanced diabetic retinopathy detection and classification approach using deep convolutional neural network", *Neural Computing and Applications*, Vol. 32, No. 3, pp. 707-721, 2020, doi: 10.1007/s00521-018-03974-0.

[6] V. Gulshan, L. Peng, M. Coram, M. C. Stumpe, D. Wu, A. Narayanaswamy, S. Venugopalan, K. Widner, T. Madams, J. Cuadros, and R. Kim, "Development and validation of a deep learning algorithm for detection of diabetic retinopathy in retinal fundus photographs", *JAMA*, Vol. 316, No. 22, pp. 2402-2410, 2016, doi: 10.1001/jama.2016.17216.

[7] R. Gargeya and T. Leng, "Automated identification of diabetic retinopathy using deep learning", *Ophthalmology*, Vol. 124, No. 7, pp. 962-969, 2017, https://doi.org/10.1016/j.ophtha.2017.02.008.

[8] A. Rakhlin, "Diabetic Retinopathy detection through integration of Deep Learning classification framework", *BioRxiv*, p. 225508, 2018, doi: 10.1101/225508.

[9] D. Le, M. Alam, C. K. Yao, J. I. Lim, Y. T. Hsieh, R. V. Chan, D. Toslak, and X. Yao, "Transfer learning for automated OCTA detection of diabetic retinopathy", *Translational Vision Science & Technology*, Vol. 9, No. 2, pp. 35-35, 2020, doi: 10.1167/tvst.9.2.35.

[10] M. T. Hagos and S. Kant, "Transfer learning based detection of diabetic retinopathy from small dataset", *arXiv Preprint arXiv:1905.07203*, 2019, doi: 10.48550/arXiv.1905.07203.

[11] M. S. Junayed, M. B. Islam, A. Sadeghzadeh, and S. Rahman, "CataractNet: An automated cataract detection system using deep learning for fundus images", *IEEE Access*, Vol. 9, pp. 128799-128808, 2021, doi: 10.1109/ACCESS.2021.3112938.

[12] T. Pratap and P. Kokil, "Computer-aided diagnosis of cataract using deep transfer learning", *Biomedical Signal Processing and Control*, Vol. 53, p. 101533, 2019, doi: 10.1016/j.bspc.2019.04.010.

[13] Y. Chai, H. Liu, and J. Xu, "Glaucoma diagnosis based on both hidden features and domain knowledge through deep learning models", *Knowledge-Based Systems*, Vol. 161, pp. 147-156, 2018, doi: 10.1016/j.knosys.2018.07.043.

[14] Q. Abbas, "Glaucoma-deep: detection of glaucoma eye disease on retinal fundus images using deep learning", *International Journal of Advanced Computer Science and Applications*, Vol. 8, No. 6, 2017.

[15] A. Markan, A. Agarwal, A. Arora, K. Bazgain, V. Rana, and V. Gupta, "Novel imaging biomarkers in diabetic retinopathy and diabetic macular edema", *Therapeutic Advances in Ophthalmology*, Vol. 12, p. 2515841420950513, 2020, doi: 10.1177/2515841420950513.

[16] R. J. Chalakkal, W. H. Abdulla, and S. C. Hong, "Fundus retinal image analyses for screening and diagnosing diabetic retinopathy, macular edema, and glaucoma disorders", *In Diabetes and Fundus OCT*, pp. 59-111, 2020, doi: 10.1016/B978-0-12-817440-1.00003-6.

[17] F. Li, Y. Wang, T. Xu, L. Dong, L. Yan, M. Jiang, X. Zhang, H. Jiang, Z. Wu, and H. Zou, "Deep learning-based automated detection for diabetic retinopathy and diabetic macular oedema in retinal fundus photographs", *Eye*, Vol. 1, pp. 1-9, 2021, doi: 10.1038/s41433-021-01552-8.

[18] A. Sungheetha and R. Sharma, "Design an early detection and classification for diabetic retinopathy by deep feature extraction based convolution neural network", *Journal of Trends in Computer Science and Smart Technology (TCSST)*, Vol. 3, No. 2, pp. 81-94, 2021, doi: 10.36548/jtcsst.2021.2.002.

[19] D. David, "Retinal image classification system for diagnosis of diabetic retinopathy using morphological edge detection and feature extraction techniques", *Artech Journal of Effective Research in Engineering and Technology*, Vol. 1, pp. 28-33, 2020.

[20] J. P. Kandhasamy, S. Balamurali, S. Kadry, and L. K. Ramasamy, "Diagnosis of diabetic retinopathy using multi-level set segmentation algorithm with feature extraction using svm with selective features", *Multimedia Tools and Applications*, Vol. 79, No. 15, pp. 10581-10596, 2020, doi: 10.1007/s11042-019-7485-8.

[21] A. Bilal, G. Sun, S. Mazhar, A. Imran, and J.

Latif, "A Transfer Learning and U-Net-based automatic detection of diabetic retinopathy from fundus images", *Computer Methods in Biomechanics and Biomedical Engineering: Imaging & Visualization*, pp. 1-12, 2022, doi: 10.1080/21681163.2021.2021111.

[22] M. Kaur and A. Kamra, "Detection of retinal abnormalities in fundus image using transfer learning networks", *Soft Computing*, Vol. 1, pp. 1-15, 2021, doi: 10.1007/s00500-021-06088-3.

[23] N. E. M. Khalifa, M. Loey, M. H. N. Taha, and H. N. E. T. Mohamed, "Deep transfer learning models for medical diabetic retinopathy detection", *Acta Informatica Medica*, Vol. 27, No. 5, p. 327, 2019, doi: 10.5455%2Faim.2019.27.327-332.

[24] A. K. Gangwar and V. Ravi, "Diabetic retinopathy detection using transfer learning and deep learning", *In Evolution in Computational Intelligence*, Vol. 1, pp. 679-689, 2021, doi: 10.1007/978-981-15-5788-0_64.

[25] M. A. Smadi, M. Hammad, Q. B. Baker, and A. Sa'ad, "A transfer learning with deep neural network approach for diabetic retinopathy classification", *International Journal of Electrical and Computer Engineering*, Vol. 11, No. 4, p. 3492, 2021, doi: 10.11591/ijece.v11i4.pp3492-3501.

[26] E. M. E. Houby, "Using transfer learning for diabetic retinopathy stage classification", *Applied Computing and Informatics*, doi: 10.1108/ACI-07-2021-0191.

[27] R. Sarki, K. Ahmed, H. Wang, Y. Zhang, and K. Wang, "Convolutional neural network for multi-class classification of diabetic eye disease", *EAI Endorsed Transactions on Scalable Information Systems*, Vol. 9, No. 4, pp. e5-e5, 2022, doi: 10.4108/eai.16-12-2021.172436.

[28] N. Gour and P. Khanna, "Multi-class multi-label ophthalmological disease detection using transfer learning based convolutional neural network", *Biomedical Signal Processing and Control*, Vol. 66, p. 102329, 2021, doi: 10.1016/j.bspc.2020.102329.

[29] W. H. Ho, T. H. Huang, P. Y. Yang, J. H. Chou, H. S. Huang, L. C. Chi, F. I. Chou, and J. T. Tsai, "Artificial intelligence classification model for macular degeneration images: a robust optimization framework for residual neural networks", *BMC Bioinformatics*, Vol. 22, pp. 1-10, 2021, doi: 10.1186/s12859-021-04085-9.

[30] R. Sarki, K. Ahmed, H. Wang, and Y. Zhang, "Automated detection of mild and multi-class diabetic eye diseases using deep learning", *Health Information Science and Systems*, Vol. 8, No. 1, p. 32, 2020, doi: 10.1007/s13755-020-00125-5.